



## Data Article

# Dataset for the dimethyl sulfoxide as a novel thermodynamic inhibitor of carbon dioxide hydrate formation

Anton P. Semenov<sup>a,\*</sup>, Rais I. Mendgaziev<sup>a</sup>, Andrey S. Stoporev<sup>a,b</sup>, Vladimir A. Istomin<sup>a,c</sup>, Daria V. Sergeeva<sup>a,c</sup>, Timur B. Tulegenov<sup>a</sup>, Vladimir A. Vinokurov<sup>a</sup>

<sup>a</sup> Gubkin University, Department of Physical and Colloid Chemistry, 65, Leninsky prospekt, Building 1, 119991, Moscow, Russian Federation

<sup>b</sup> Nikolaev Institute of Inorganic Chemistry SB RAS, Ac. Lavrentiev ave. 3, 630090, Novosibirsk, Russian Federation

<sup>c</sup> Skolkovo Institute of Science and Technology (Skoltech), Nobelya Str. 3, 121205, Moscow, Russian Federation

## ARTICLE INFO

## Article history:

Received 22 April 2022

Revised 9 May 2022

Accepted 12 May 2022

Available online 17 May 2022

Dataset link: [Raw data of CO<sub>2</sub> hydrate equilibrium conditions measurements in the CO<sub>2</sub> – H<sub>2</sub>O – dimethyl sulfoxide system \(Original data\)](#)

## Keywords:

Gas hydrates

Carbon dioxide

Gas hydrate inhibitor

Dimethyl sulfoxide

Phase equilibria

## ABSTRACT

The temperatures and pressures of the three-phase equilibrium V-L<sub>w</sub>-H (gas – aqueous solution – gas hydrate) were measured in the CO<sub>2</sub> – H<sub>2</sub>O – dimethyl sulfoxide (DMSO) system at concentrations of organic solute in the aqueous phase up to 50 mass%. Measurements of CO<sub>2</sub> hydrate equilibrium conditions were carried out using a constant volume autoclave by continuous heating at a rate of 0.1 K/h with simultaneous stirring of fluids by a four-blade agitator at 600 rpm. The equilibrium temperature and pressure of CO<sub>2</sub> hydrate were determined for the endpoint of the hydrate dissociation in each experiment. The CO<sub>2</sub> gas fugacity was calculated by the equation of state for carbon dioxide for the measured points. The flow regime in the autoclave during the operation of the stirring system was characterized by calculating the Reynolds number using literature data on the viscosity and density of water and DMSO aqueous solutions. We employed regression analysis to approximate the dependences of equilibrium pressure (CO<sub>2</sub> gas fugacity) on temperature by two- and three-parameter equations. For each measured

DOI of original article: [10.1016/j.ces.2022.117670](https://doi.org/10.1016/j.ces.2022.117670)

\* Corresponding author.

E-mail address: [semenov.a@gubkin.ru](mailto:semenov.a@gubkin.ru) (A.P. Semenov).

<https://doi.org/10.1016/j.dib.2022.108289>

2352-3409/© 2022 The Authors. Published by Elsevier Inc. This is an open access article under the CC BY-NC-ND license (<http://creativecommons.org/licenses/by-nc-nd/4.0/>)

point, the value of CO<sub>2</sub> hydrate equilibrium temperature suppression  $\Delta T_h$  was computed. The dependences of this quantity on CO<sub>2</sub> gas fugacity are considered for all DMSO concentrations. The coefficients of empirical correlation describing  $\Delta T_h$  as a function of the DMSO mass fraction in solution and the equilibrium gas pressure are determined.

This article is a co-submission with a paper [1].

© 2022 The Authors. Published by Elsevier Inc.

This is an open access article under the CC BY-NC-ND license (<http://creativecommons.org/licenses/by-nc-nd/4.0/>)

## Specifications Table

Subject	Chemistry
Specific subject area	Physical and Theoretical Chemistry
Type of data	Tables, figures
How the data were acquired	Equilibrium conditions of three-phase coexistence V-L <sub>w</sub> -H (CO <sub>2</sub> gas – DMSO aqueous solution – CO <sub>2</sub> hydrate) were experimentally measured by an isochoric method with slow heating at a rate of 0.1 K/h. Gas hydrate autoclave GHA350 (PSL Systemtechnik, Germany) with a volume of 600 mL equipped with calibrated pressure, temperature sensors, stirring, and temperature control system was employed. The equilibrium temperature and pressure were determined for the endpoint of the gas hydrate dissociation, in which there was an abrupt decrease in the slope of the dependence of pressure on temperature during slow heating (0.1 K/h) and intensive stirring of the system (600 rpm). The autoclave stirring system includes an agitator with the geometry of a four-blade propeller, magnetic coupling Minipower (Premex, Switzerland), and an overhead stirrer Hei-TORQUE 400 Precision (Heidolph, Germany). The temperature control system consists of an outer jacket of the autoclave, to which a circulation thermostat CC 505 (Huber, Germany) is attached, filled with ethanol as a coolant. A personal computer with WinGHA software is used to automatically control the operation of the setup and record data. Experimental data processing and visualization were carried out using the OriginPro 2020b package.
Data format	Raw and analyzed
Description of data collection	Measurements of the CO <sub>2</sub> hydrate equilibrium conditions were made for the aqueous solutions of DMSO with the following mass fractions of organic solute: 0, 5, 10, 20, 30, 40, 45, and 50 mass%. The ratio of the free volume in the autoclave to the volume of the liquid phase was 1:1. Experimental data were obtained in the temperature range 243 – 283 K.
Data source location	Gubkin University, Department of Physical and Colloid Chemistry, Moscow, Russia. 55.692232°N, 37.55487°E
Data accessibility	Repository name: Mendeley Data Data identification number: 10.17632/5xjdgvyjb84.1 Direct URL to data: <a href="https://data.mendeley.com/datasets/5xjdgvyjb84/1">https://data.mendeley.com/datasets/5xjdgvyjb84/1</a>
Related research article	A.P. Semenov, R.I. Mendgaziev, A.S. Stoporev, V.A. Istomin, D. V. Sergeeva, T.B. Tulegenov, V.A. Vinokurov, Dimethyl sulfoxide as a novel thermodynamic inhibitor of carbon dioxide hydrate formation. Chem. Eng. Sci. 255 (2022) 117670. <a href="https://doi.org/10.1016/j.ces.2022.117670">https://doi.org/10.1016/j.ces.2022.117670</a> [1].

## Value of the Data

- The obtained data allow predicting the phase boundaries of carbon dioxide hydrate in the CO<sub>2</sub> – H<sub>2</sub>O and CO<sub>2</sub> – H<sub>2</sub>O – DMSO systems.
- One can use the data as a reference for working off the methodology for measuring the equilibrium conditions of hydrate formation as well as for a comparative evaluation of the

effectiveness of DMSO and other thermodynamic inhibitors both in laboratory studies and in solving applied problems related to the inhibition of gas hydrate formation.

- The data can be integrated into software for automated calculation of the CO<sub>2</sub> hydrate equilibrium conditions and prediction of DMSO consumption for gas hydrate inhibition under specific conditions.

## 1. Data Description

To characterize the flow regime induced by the function of the autoclave's stirring system we calculated dimensionless coefficient, Reynolds number  $Re$ , from the equation 3.1 ref. [2]. The necessary density and viscosity values for DMSO – water solutions were taken from the literature (Supplementary in ref. [3]). Substituting into the formula for the Reynolds number also requires agitator diameter and stirring frequency, which in our case are equal to 0.061 m and 10 s<sup>-1</sup>, respectively. The calculation data are reported in Table 1 and Fig. 1.

Table 2 contains the measured values of equilibrium pressure and temperature for each DMSO concentration. The experimental pressure and temperature trajectories from which the equilibrium values were determined in each experiment can be found at the above link to the Mendeleev Data repository. Along with the measured data Table 2 contains CO<sub>2</sub> gas fugacities calculated for every equilibrium point according to GERG-2008 equation of state [4]. Carbon dioxide hydrate equilibrium curves for CO<sub>2</sub> – H<sub>2</sub>O – DMSO system in gas fugacity – temperature coordinates are depicted in Fig. 2. To describe the hydrate dissociation data, we used Eq. 1 [5,6]:

$$\ln P(\text{or } f) = A + \frac{B}{T}, \quad (1)$$

**Table 1**

Calculated Reynolds number  $Re$  values for stirring of water and DMSO aqueous solutions in the autoclave GHA350 at the rate of 600 rpm (using eq.3.1 from ref. [2]); density and viscosity values are taken from Supplementary data of ref. [3]

$\omega_{\text{DMSO}}$ in water solution, mass% <sup>a</sup>	$T, \text{K}$ <sup>b</sup>	density $\rho$ , kg/m <sup>3</sup> <sup>c</sup>	dynamic viscosity $\eta \cdot 10^3$ , kg/(m·s) <sup>d</sup>	Reynolds number $Re$
I	II	III	IV	V
0 (pure water)	293.15	998.21	0.998	37210
	283.15	999.70	1.296	28711
	273.15	999.90	1.792	20765
10.01	293.15	1011.22	1.236	30450
	283.15	1013.51	1.631	23126
	273.15	1014.73	2.268	16649
20.00	293.15	1025.44	1.548	24642
	283.15	1028.76	2.073	18467
	273.15	1031.29	2.914	13167
30.00	293.15	1040.70	1.977	19584
	283.15	1045.16	2.683	14496
	273.15	1049.08	3.821	10217
40.00	293.15	1056.64	2.551	15414
	283.15	1062.26	3.524	11218
	273.15	1067.51	5.111	7772
50.00	293.15	1072.37	3.259	12244
	283.15	1079.08	4.587	8753
	273.15	1085.54	6.771	5966

<sup>a</sup> Expanded uncertainty of DMSO mass fraction (except for pure water) is 0.012 mass% ( $k = 2$ ).

<sup>b</sup> Expanded uncertainty of temperature is 0.02 K ( $k = 2$ ) for density and viscosity measurements by density meter DMA 4500 coupled with viscometer Lovis 2000 ME (Anton Paar, Austria).

<sup>c</sup> Expanded uncertainty is 0.05 kg/m<sup>3</sup> ( $k = 2$ ).

<sup>d</sup> Expanded uncertainty is 0.5% of dynamic viscosity value ( $k = 2$ ).

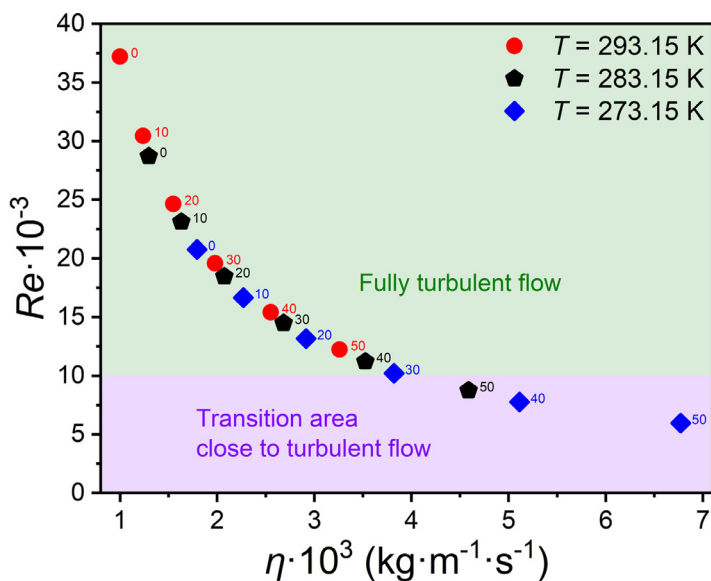


**Fig. 1.** Reynolds number (column V in Table 1) as a function of dynamic viscosity of liquid phase (column IV in Table 1) for stirring of water and DMSO aqueous solutions in the autoclave GHA350 at the rate of 600 rpm; numbers to the right of the points show the mass fraction of DMSO in water solution; olive- and violet-filled areas correspond to regions of fully turbulent flow ( $Re > 10000$ ) and transition area close to turbulent flow ( $30 < Re < 10000$ ), respectively.

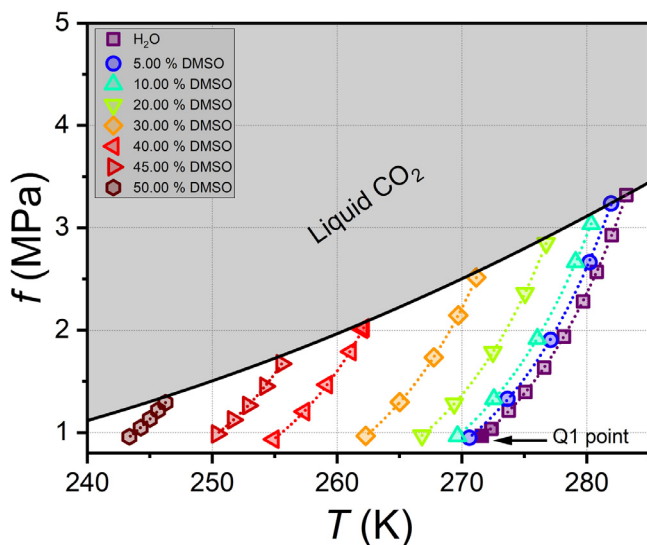


**Fig. 2.** Three-phase V-L<sub>w</sub>-H equilibrium conditions for CO<sub>2</sub> - H<sub>2</sub>O - DMSO system measured in this work (markers) in fugacity - temperature coordinates (columns VI and IV in Table 2); the lowest point for pure H<sub>2</sub>O is the quadruple point Q1 [8]; black solid curve shows saturated vapor fugacity of pure CO<sub>2</sub> [9]; dotted curves are approximations by exponential form of equation 2; grey- and white-filled areas correspond to regions of liquid and gaseous CO<sub>2</sub>; (mass fractions of DMSO in solution are shown in the legend).

**Table 2**

Experimental data on V-L<sub>w</sub>-H equilibrium conditions for the system of CO<sub>2</sub> – H<sub>2</sub>O – DMSO and calculated values of CO<sub>2</sub> gas fugacity by GERG-2008 equation of state [4]

# of system	Initial composition of DMSO – water solution, mass% (mol%) <sup>a</sup>	# of point	T, K <sup>b</sup>	P, MPa <sup>c</sup>	CO <sub>2</sub> gas fugacity <i>f</i> , MPa
I	II	III	IV	V	VI
1	0 (pure water)	-	271.60 <sup>d</sup>	1.04 <sup>d</sup>	0.9676
		1	272.35	1.12	1.0368
		2	272.37	1.12	1.0368
		3	273.74	1.33	1.2147
		4	275.08	1.55	1.3961
		5	276.58	1.85	1.6349
		6	278.17	2.25	1.9381
		7	279.70	2.73	2.2795
		8	280.79	3.17	2.5705
		9	281.99	3.76	2.9275
2	5.00 (1.20)	10	283.16 <sup>e</sup>	4.52 <sup>e</sup>	3.3207
		11	270.59	1.02	0.9494
		12	273.64	1.47	1.3291
		13	277.09	2.21	1.9051
		14	280.21	3.33	2.6635
3	10.00 (2.50)	15	281.94 <sup>e</sup>	4.37 <sup>e</sup>	3.2385
		16	269.65	1.04	0.9658
		17	272.56	1.47	1.3272
		18	276.04	2.23	1.9156
4	20.00 (5.45)	19	279.10	3.35	2.6661
		20	280.35	4.00	3.0365
		21	266.80	1.05	0.9717
		22	269.38	1.42	1.2814
		23	272.48	2.07	1.7870
		24	275.06	2.90	2.3618
		25	276.74	3.72	2.8491
5	30.00 (8.99)	26	262.30	1.05	0.9672
		27	265.02	1.45	1.2975
		28	267.74	2.02	1.7342
		29	269.70	2.61	2.1440
		30	271.15	3.21	2.5158
6	40.00 (13.32)	31	254.92	1.02	0.9341
		32	257.36	1.35	1.2042
		33	259.18	1.69	1.4669
		34	261.09	2.14	1.7906
		35	262.02	2.47	2.0093
		36	262.13	2.49	2.0224
		37	250.38	1.09	0.9858
7	45.00 (15.87)	38	251.67	1.26	1.1232
		39	252.88	1.44	1.2641
		40	254.25	1.69	1.4519
		41	255.56	2.00	1.6719
8	50.00 (18.74)	42	243.37	1.07	0.9596
		43	244.28	1.18	1.0474
		44	245.01	1.29	1.1330
		45	245.66	1.40	1.2167
		46	246.26	1.50	1.2912

<sup>a</sup> Expanded uncertainty of DMSO mass fraction is 0.012 mass% ( $k = 2$ )

<sup>b</sup> Expanded uncertainty is 0.1 K ( $k = 2$ )

<sup>c</sup> Expanded uncertainty is 0.02 MPa ( $k = 2$ )

<sup>d</sup> Literature data on quadruple point (four-phase V-L<sub>w</sub>-H equilibrium) for CO<sub>2</sub> – H<sub>2</sub>O system [8]

<sup>e</sup> Traces of liquid CO<sub>2</sub> could be present in the system

**Table 3**  
Fit (eq.1) of experimental data on CO<sub>2</sub> hydrate equilibrium conditions

#	Initial composition of DMSO – water mixture, mass% (mol%) of DMSO	A		B, K		Adjusted R <sup>2</sup> or $\bar{R}^2$
		Value	Standard Error	Value	Standard Error	
I	II	III	IV	V	VI	VII
<b>for equilibrium pressure of CO<sub>2</sub> gas</b>						
1	0 (0)	35.41	0.64	-9615.53	176.47	0.9966
2	5.00 (1.20)	35.77	1.14	-9680.24	314.49	0.9958
3	10.00 (2.50)	35.13	0.82	-9465.82	227.20	0.9977
4	20.00 (5.45)	35.02	0.95	-9335.93	259.28	0.9969
5	30.00 (8.99)	34.14	0.81	-8946.84	215.78	0.9977
6	40.00 (13.32)	32.63	0.72	-8315.79	185.91	0.9975
7	45.00 (15.87)	30.14	0.63	-7528.18	158.77	0.9982
8	50.00 (18.74)	29.45	0.67	-7151.85	163.38	0.9979
<b>for equilibrium fugacity of CO<sub>2</sub> gas</b>						
1	0 (0)	30.23	0.16	-8223.36	43.39	0.9997
2	5.00 (1.20)	30.26	0.28	-8202.60	78.74	0.9996
3	10.00 (2.50)	29.97	0.15	-8092.26	41.15	0.9999
4	20.00 (5.45)	29.86	0.26	-7976.31	71.94	0.9997
5	30.00 (8.99)	29.19	0.21	-7667.00	56.20	0.9998
6	40.00 (13.32)	28.13	0.34	-7190.51	87.52	0.9993
7	45.00 (15.87)	25.92	0.33	-6494.62	82.74	0.9994
8	50.00 (18.74)	25.49	0.39	-6214.55	94.59	0.9991

where A, B – adjusted parameters, P or f – equilibrium pressure or fugacity (MPa), T – equilibrium temperature (K). The numerical values of the adjusted parameters are tabulated in Table 3. Figs. 3 and 4 show the approximation data of equilibrium conditions for CO<sub>2</sub> hydrate in pressure and fugacity coordinates, respectively.

We also tested a three-parameter model (eq. 2) to approximate experimental data on CO<sub>2</sub> hydrate equilibria.

$$\ln P \text{ (or } f) = A + \frac{B}{T} + C \times \ln T \tag{2}$$

The main difference between this model from the two-parameter one (eq. 1) is the presence of the third term, which is the product of the coefficient C and the logarithmic equilibrium temperature. The numerical values of coefficients of this model are tabulated in Table 4. The approximations are shown in Figs. 5 and 6.

Suppression of CO<sub>2</sub> hydrate equilibrium temperature as a function of gas fugacity for each inhibitor concentration is presented in Fig. 7. Surface fitting of our experimental data on suppression of CO<sub>2</sub> hydrate equilibrium temperature ΔT<sub>h</sub> as a function of DMSO solution concentration and gas pressure by known equations [3,7] are reported in Fig. 8, Table 5, and Fig. 9 of the original research paper [1].

## 2. Experimental Design, Materials and Methods

Carbon dioxide (>99.99 vol% purity, NIIKM, Moscow, Russia), dimethyl sulfoxide (>99.8 mass% purity, ECOS-1, Moscow, Russia), and deionized water from the in-house system (18.2 MΩ·cm, Simplicity UV, Millipore) were used. Dimethyl sulfoxide was used as received from the supplier. To control the purity, we measured the refractive indices on the sodium D-line for DMSO and water at a temperature of 293.15 K (Abbemat 650 refractometer, Anton Paar), which were 1.479376±0.000001 and 1.332990±0.000001, respectively. 300 mL aqueous solution of DMSO at the specified concentration for each series of experiments was prepared gravimet-

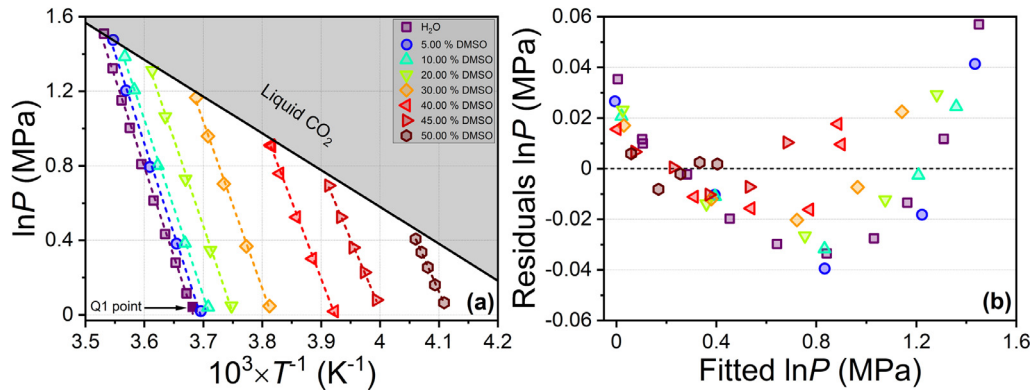


**Fig. 3.** (a) Logarithmic equilibrium CO<sub>2</sub> pressures as functions of the reciprocal equilibrium temperatures, markers are experimental points, dashed lines are linear fits (eq. 1); the lowest point for pure H<sub>2</sub>O is the quadruple point Q1 [8]; solid black line shows saturated vapor pressure of pure CO<sub>2</sub> [9], grey- and white-filled areas (a) correspond to regions of liquid and gaseous CO<sub>2</sub>; mass fractions of DMSO are shown in the legend; (b) residuals of linear fit as a function of the fitted value of the logarithmic equilibrium pressure.

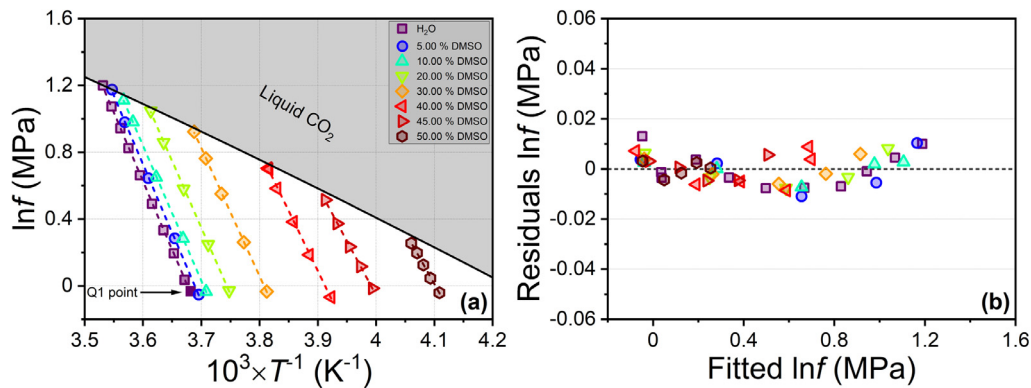


**Fig. 4.** (a) Logarithmic equilibrium  $\text{CO}_2$  fugacities as functions of the reciprocal equilibrium temperatures, markers are experimental points, dashed lines are linear fits (eq. 1); the lowest point for pure  $\text{H}_2\text{O}$  is the quadruple point Q1 [8]; solid black line shows saturated vapor fugacity of pure  $\text{CO}_2$  [9], grey- and white-filled areas (a) correspond to regions of liquid and gaseous  $\text{CO}_2$ ; mass fractions of DMSO are shown in the legend; (b) residuals of linear fit as a function of the fitted value of the logarithmic equilibrium fugacity.

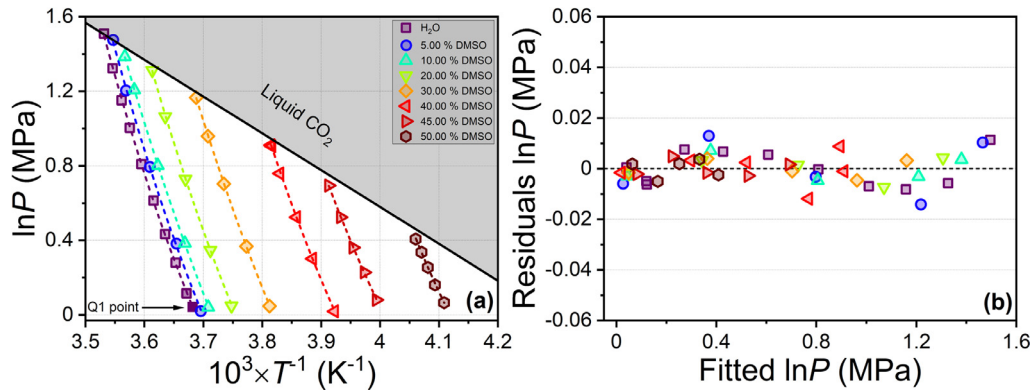


**Fig. 5.** (a) Logarithmic equilibrium CO<sub>2</sub> pressures as functions of the reciprocal equilibrium temperatures, markers are experimental points, dashed lines are fits (eq. 2); the lowest point for pure H<sub>2</sub>O is the quadruple point Q1 [8]; solid black line shows saturated vapor pressure of pure CO<sub>2</sub> [9], grey- and white-filled areas (a) correspond to regions of liquid and gaseous CO<sub>2</sub>; mass fractions of DMSO are shown in the legend; (b) residuals of fit as a function of the fitted value of the logarithmic equilibrium pressure.

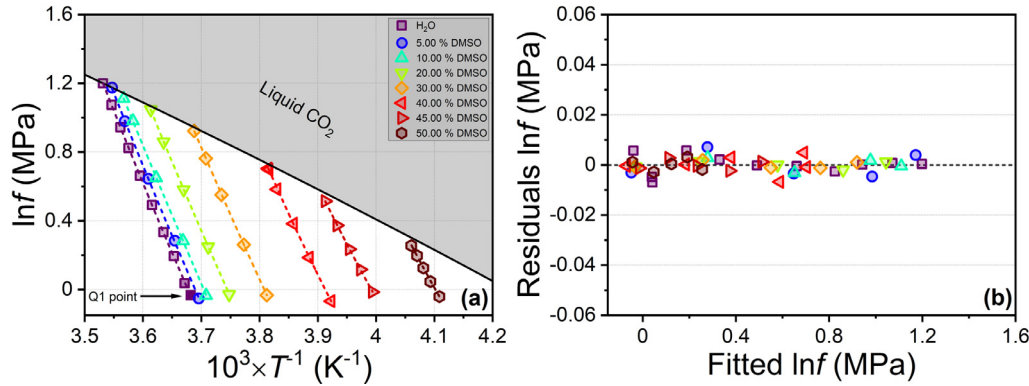


**Fig. 6.** (a) Logarithmic equilibrium  $\text{CO}_2$  fugacities as functions of the reciprocal equilibrium temperatures, markers are experimental points, dashed lines are fits (eq. 2); the lowest point for pure  $\text{H}_2\text{O}$  is the quadruple point Q1 [8]; solid black line shows saturated vapor fugacity of pure  $\text{CO}_2$  [9], grey- and white-filled areas (a) correspond to regions of liquid and gaseous  $\text{CO}_2$ ; mass fractions of DMSO are shown in the legend; (b) residuals of fit as a function of the fitted value of the logarithmic equilibrium fugacity.

**Table 4**Fit (eq.2) of experimental data on CO<sub>2</sub> hydrate equilibrium conditions

Initial composition of DMSO – water mixture, mass% (mol%) of DMSO		A		B, K		C		Adjusted $R^2$ or $\bar{R}^2$
		Value	Standard Error	Value	Standard Error	Value	Standard Error	
#		III	IV	V	VI	VII	VIII	IX
<b>for equilibrium pressure of CO<sub>2</sub> gas</b>								
1	0 (0)	-2280.30	203.02	87247.95	8492.34	349.57	30.65	0.9998
2	5.00 (1.20)	-2149.53	564.05	81483.04	23530.59	330.04	85.19	0.9993
3	10.00 (2.50)	-1752.65	284.76	64834.94	11834.90	270.18	43.04	0.9998
4	20.00 (5.45)	-2106.87	293.06	78778.16	12056.25	324.29	44.37	0.9998
5	30.00 (8.99)	-1910.18	265.84	69775.92	10763.51	295.22	40.36	0.9999
6	40.00 (13.32)	-2162.48	608.27	78298.58	24001.33	334.84	92.79	0.9994
7	45.00 (15.87)	-2148.82	607.40	76838.25	23517.68	333.52	92.97	0.9996
8	50.00 (18.74)	-3104.60	2027.83	110873.92	76366.44	482.13	311.95	0.9986
<b>for equilibrium fugacity of CO<sub>2</sub> gas</b>								
1	0 (0)	-459.26	114.34	12251.31	4782.63	73.89	17.26	0.9999
2	5.00 (1.20)	-424.60	257.21	10772.42	10730.19	68.70	38.85	0.9998
3	10.00 (2.50)	-244.07	132.39	3297.22	5502.06	41.42	20.01	1.0000
4	20.00 (5.45)	-562.73	87.36	16402.00	3593.84	89.72	13.23	1.0000
5	30.00 (8.99)	-464.48	105.68	12320.91	4279.00	74.96	16.05	1.0000
6	40.00 (13.32)	-944.60	350.13	31191.60	13815.66	148.38	53.41	0.9997
7	45.00 (15.87)	-1065.97	385.77	35781.81	14936.38	167.13	59.05	0.9998
8	50.00 (18.74)	-1549.98	1335.35	53116.28	50288.29	242.36	205.42	0.9992

**Table 5**Two fits of data on suppression of CO<sub>2</sub> hydrate equilibrium temperature  $\Delta T_h$  as a function of DMSO concentration (0 – 50 mass%) and pressure in the system (from 1 MPa to saturated vapor pressure of pure CO<sub>2</sub> in the temperature range of 243 – 283 K)

Coefficient	Østergaard correlation (eq.1 in ref. [7])	Our correlation (eq. 4 from ref. [3])
$b_1$	96.3637122	1693.3200948
$b_2$	-1.5341795	79.0155118
$b_3$	0.0840859	-1.7438853
$b_4$	0.0145624	0.0426424
$b_5$	$1.7315494 \cdot 10^{-4}$	$8.6317033 \cdot 10^{-5}$
$b_6$	-0.8313092	$-8.1550684 \cdot 10^{-7}$
$b_7$	-	$5.1541498 \cdot 10^{-7}$
$\bar{R}^2$	0.99965	0.99994
Average absolute deviation (K) (equation 5 from ref. [3])	0.18	0.07
Average absolute relative deviation (%) (equation 6 from ref. [3])	4.49	1.59

rically in a 500 mL Erlenmeyer flask. The masses of the components were measured using calibrated balances PA413C (Ohaus Pioneer, USA) with a resolution of 0.001 g and maximum error  $\pm 0.01$  g.

Gas hydrate autoclave GHA350 (PSL Systemtechnik, Germany) with a volume of 600 mL equipped with calibrated pressure, Pt100 temperature sensors (errors are  $\pm 0.02$  MPa and  $\pm 0.1$  K), stirring, and temperature control system was employed. The autoclave stirring system includes an agitator with the geometry of a four-blade propeller (diameter 0.061 m), magnetic coupling Minipower (Premex, Switzerland), and an overhead stirrer Hei-TORQUE 400 Precision (Heidolph, Germany). The temperature control system consists of an outer jacket of the autoclave, to which a circulation thermostat CC 505 (Huber, Germany) is attached, filled with ethanol as a coolant. The possible range of temperature in the autoclave when using ethanol and the CC 505 thermostat is 230 – 303 K. This thermostat ensures the stability of temperature in the autoclave of  $\pm 0.02$  K. Before experiments, the GHA350 temperature and pressure sensors

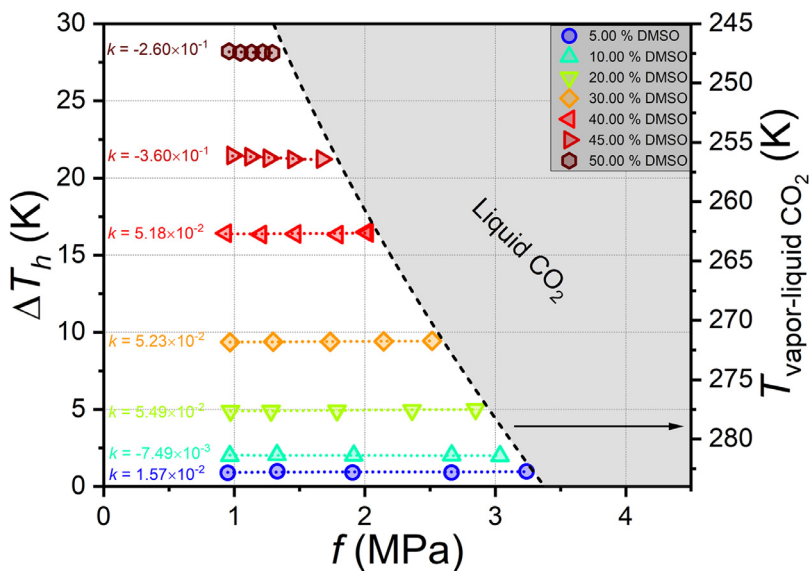


**Fig. 7.** Suppression of CO<sub>2</sub> hydrate equilibrium temperature as a function of gas fugacity (left Y axis); markers and dotted lines correspond to experimental points and linear regressions, respectively; for each concentration, the values of slope  $k$  are depicted; dashed black line shows saturated vapor fugacity of pure CO<sub>2</sub> [9] (right Y axis), grey- and white-filled areas correspond to regions of liquid and gaseous CO<sub>2</sub>; concentrations of DMSO in the legend are in mass%.

were calibrated using reference measuring instruments. A detailed description of the calibration procedure can be found elsewhere [3]. A personal computer with WinGHA software (version 4.0.10.790) is used to automatically control the operation of the setup and record data.

The resulting aqueous solution of DMSO was placed in the autoclave, the free volume of which was further purged with gaseous carbon dioxide three times by increasing the pressure to 1 MPa and then dropping to the atmospheric level. Gaseous carbon dioxide was then supplied, and the aqueous solution was saturated with gas at a temperature of 294 K until the required pressure was reached with stirring on (600 rpm). Carbon dioxide hydrate formation was induced by cooling the autoclave at a rate of 5 K/h. Carbon dioxide hydrate crystallization leads to sudden pressure drop and temperature rise due to exothermic effect. Then the autoclave was heated to a temperature 0.5 – 1 K lower than the equilibrium value, which led to the decomposition of the main amount of the CO<sub>2</sub> hydrate phase. The system was kept for 6 – 7 hours. During this time, the temperature and pressure in the autoclave reached a plateau. Equilibrium conditions of three-phase coexistence V-L<sub>w</sub>-H (CO<sub>2</sub> gas – DMSO aqueous solution – CO<sub>2</sub> hydrate) were measured by an isochoric method with slow heating at a rate of 0.1 K/h. The equilibrium temperature and pressure were determined for the endpoint of the gas hydrate dissociation, in which there was an abrupt decrease in the slope of the dependence of pressure on temperature during slow heating (0.1 K/h) and intensive stirring of the system (600 rpm) [10,11]. Experimental data processing and visualization were carried out using the OriginPro 2020b package.

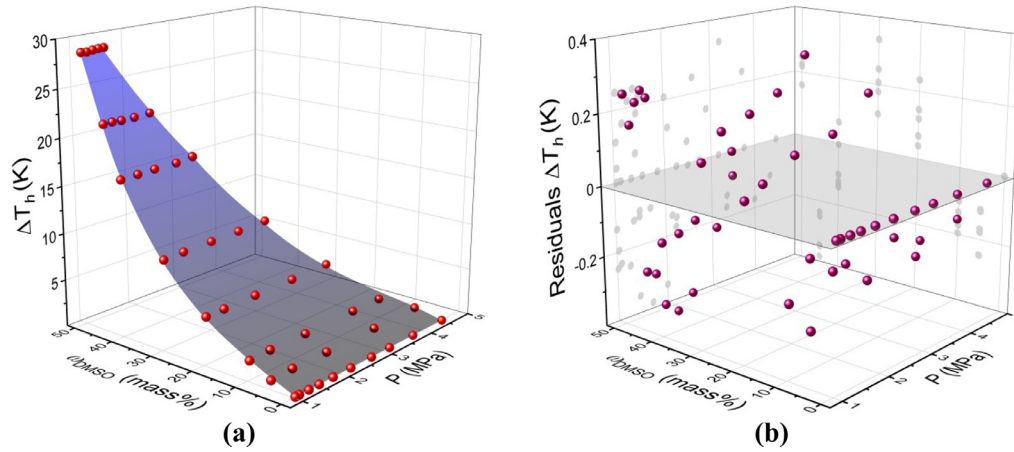


**Fig. 8.** (a) Suppression of CO<sub>2</sub> hydrate equilibrium temperature  $\Delta T_h$  as a function of DMSO solution concentration and gas pressure, markers are experimental data, surface is approximation by Østergaard *et al.* model (eq. 1 from ref. [7]); (b) markers are fit residuals of  $\Delta T_h$  (difference between experimental and fitted value for each point).

## Ethics Statements

The studies described in the manuscript were conducted adhering to Ethics in publishing standards (<https://www.elsevier.com/journals/data-in-brief/2352-3409/guide-for-authors>) and did not involve human or animal subjects.

## CRediT Author Statement

**Anton P. Semenov:** Data curation, Visualization, Writing – original draft preparation, Validation, Writing – review & editing, Project administration, Funding acquisition; **Rais I. Mendgaziev:** Investigation, Data curation; **Andrey S. Stoporev:** Investigation, Visualization, Writing – original draft preparation, Writing – review & editing; **Vladimir A. Istomin:** Data curation, Writing – review & editing; **Daria V. Sergeeva:** Data curation; **Timur B. Tulegenov:** Investigation; **Vladimir A. Vinokurov:** Resources, Supervision.

## Declaration of Competing Interest

The authors declare that they have no known competing financial interests or personal relationships that could have appeared to influence the work reported in this paper.

## Data Availability

[Raw data of CO<sub>2</sub> hydrate equilibrium conditions measurements in the CO<sub>2</sub> – H<sub>2</sub>O – dimethyl sulfoxide system \(Original data\)](#) (Mendeley Data)

## Acknowledgments

Funding: This work was supported by the Russian Science Foundation (grant 20-79-10377).

## References

- [1] A.P. Semenov, R.I. Mendgaziev, A.S. Stoporev, V.A. Istomin, D.V. Sergeeva, T.B. Tulegenov, V.A. Vinokurov, Dimethyl sulfoxide as a novel thermodynamic inhibitor of carbon dioxide hydrate formation, *Chem. Eng. Sci.* 255 (2022) 117670, doi:[10.1016/j.ces.2022.117670](https://doi.org/10.1016/j.ces.2022.117670).
- [2] F.S. Merkel, C. Schmuck, H.J. Schultz, Investigation of the influence of hydroxyl groups on gas hydrate formation at pipeline-like conditions, *Energy and Fuels* 30 (2016) 9141–9149, doi:[10.1021/acs.energyfuels.6b01795](https://doi.org/10.1021/acs.energyfuels.6b01795).
- [3] A.P. Semenov, R.I. Mendgaziev, A.S. Stoporev, V.A. Istomin, D.V. Sergeeva, A.G. Ogienko, V.A. Vinokurov, The pursuit of a more powerful thermodynamic hydrate inhibitor than methanol. Dimethyl sulfoxide as a case study, *Chem. Eng. J.* (2021) 130227, doi:[10.1016/j.cej.2021.130227](https://doi.org/10.1016/j.cej.2021.130227).
- [4] O. Kunz, W. Wagner, The GERG-2008 wide-range equation of state for natural gases and other mixtures: an expansion of GERG-2004, *J. Chem. Eng. Data.* 57 (2012) 3032–3091, doi:[10.1021/jc300655b](https://doi.org/10.1021/jc300655b).
- [5] E. Heidaryan, M.D. Robustillo Fuentes, P. de A. Pessoa Filho, Equilibrium of methane and carbon dioxide hydrates below the freezing point of water: literature review and modeling, *J. Low Temp. Phys.* 194 (2019) 27–45, doi:[10.1007/s10909-018-2049-2](https://doi.org/10.1007/s10909-018-2049-2).
- [6] A.P. Semenov, V.I. Medvedev, P.A. Gushchin, V.S. Yakushev, Effect of heating rate on the accuracy of measuring equilibrium conditions for methane and argon hydrates, *Chem. Eng. Sci.* (2015) 137, doi:[10.1016/j.ces.2015.06.031](https://doi.org/10.1016/j.ces.2015.06.031).
- [7] K.K. Østergaard, R. Masoudi, B. Tohidi, A. Danesh, A.C. Todd, A general correlation for predicting the suppression of hydrate dissociation temperature in the presence of thermodynamic inhibitors, *J. Pet. Sci. Eng.* 48 (2005) 70–80, doi:[10.1016/j.petrol.2005.04.002](https://doi.org/10.1016/j.petrol.2005.04.002).
- [8] Y. Nema, R. Ohmura, I. Senaha, K. Yasuda, Quadruple point determination in carbon dioxide hydrate forming system, *Fluid Phase Equilib* 441 (2017) 49–53, doi:[10.1016/j.fluid.2016.12.014](https://doi.org/10.1016/j.fluid.2016.12.014).
- [9] W. Duschek, R. Kleinrahm, W. Wagner, Measurement and correlation of the (pressure, density, temperature) relation of carbon dioxide II. Saturated-liquid and saturated-vapour densities and the vapour pressure along the entire coexistence curve, *J. Chem. Thermodyn.* 22 (1990) 841–864, doi:[10.1016/0021-9614\(90\)90173-N](https://doi.org/10.1016/0021-9614(90)90173-N).

- [10] A.P. Semenov, A.S. Stoporev, R.I. Mendgaziev, P.A. Gushchin, V.N. Khlebnikov, V.S. Yakushev, V.A. Istomin, D.V. Sergeeva, V.A. Vinokurov, Synergistic effect of salts and methanol in thermodynamic inhibition of sII gas hydrates, *J. Chem. Thermodyn.* 137 (2019) 119–130, doi:[10.1016/j.jct.2019.05.013](https://doi.org/10.1016/j.jct.2019.05.013).
- [11] A.P. Semenov, V.I. Medvedev, P.A. Gushchin, M.S. Kotelev, V.S. Yakushev, A.S. Stoporev, A.A. Sizikov, A.G. Ogienko, V.A. Vinokurov, Phase equilibrium for clathrate hydrate formed in methane + water + ethylene carbonate system, *Fluid Phase Equilib* 432 (2017) 1–9, doi:[10.1016/j.fluid.2016.10.015](https://doi.org/10.1016/j.fluid.2016.10.015).